

## EFFECT OF COPPER ADDITION ON THE MICROSTRUCTURE, MECHANICAL, THERMAL, AND MAGNETIC PROPERTIES OF Fe-Ni-Cu ALLOYS

Serdar Delice <sup>\*</sup>, Hakan Gungunes

Hitit University, Faculty of Engineering and Natural Sciences, Department of Physics, Çorum, Turkey

(Received 21 July 2025; Accepted 29 October 2025)

### Abstract

In this study, FeNiCu alloys with two different copper contents were produced by arc melting. The aim was to investigate the effects of Cu content on the microstructural, mechanical, thermal, and Mössbauer properties of the alloys. Microstructures were examined using SEM micrographs. Vickers hardness tests were conducted to evaluate mechanical strength. Thermal behavior was analyzed using DSC. Magnetic characteristics were studied by Mössbauer spectroscopy. SEM analysis showed the presence of martensitic structures in both alloys, with the alloy containing more Cu exhibiting a higher amount of martensite. Hardness increased from 169.1 HV to 190.2 HV as Cu content increased. DSC results confirmed the martensitic transformation. The alloy with higher Cu content showed a higher transformation temperature and greater transformation energy released. Mössbauer spectra indicated the presence of both magnetically ordered and non-ordered phases in both alloys. Hyperfine parameters demonstrated changes in the local atomic environment due to Cu addition. The weak singlet obtained was associated with the FCC phase. The two sextets were attributed to ferromagnetic BCC phases arising from different environments of the Fe atom. The other sextet, with a low internal magnetic field of around 18 T, was ascribed to possible Ni- and/or Cu-rich surroundings of the Fe atom. Overall, increasing Cu in the alloy altered the microstructure, improved hardness, shifted the martensitic transformation temperature, and modified the magnetic hyperfine interactions. These results may aid in designing advanced Fe-based materials for structural and magnetic applications.

**Keywords:** FeNiCu; SEM; Vickers Hardness; DSC; Mössbauer effect

### 1. Introduction

Iron (Fe) based alloys represent a significant class of materials characterized by their mechanical robustness, magnetic efficiency, and versatility for various applications. These alloys can incorporate elements such as Co, Ni, Cr and Mn, which enhance specific properties related to various applications [1-3]. Among them, FeNi alloys have been mostly studied for their unique properties [4, 5]. These alloys are a class of ferromagnetic materials that have taken significant attention due to their unique properties and wide range of applications [6]. FeNi alloys can exhibit both face-centered cubic (FCC) and body-centered cubic (BCC) crystal structures, depending on the composition and processing conditions [7-9]. The FCC crystal structure is more commonly observed in FeNi alloys, especially at higher Ni contents (above 30 at.%) [7, 8]. The BCC crystal structure can be stabilized in FeNi alloys, particularly at lower Ni contents (below 25 at.%) [9]. For the Ni content

ranging from 25 at.% to 30 at.%, mixed phase comprising both BCC and FCC phases occur in Fe-Ni alloys [10]. Moreover, according to literature works, the Fe-Ni alloys with Ni concentration of 36 at.% present the properties of the Invar alloys [10, 11]. However, the Fe-Ni alloys with the Ni concentration in between 30 at.% and 45 at.% are accepted to be the Invar since they show the Invar behavior [11]. The microstructural evolution and mechanical properties of FeNi alloys can be influenced by the addition of other alloying elements, such as Cr, Al, and Cu. Studies have indicated that the  $AlCoCr_xFeNi_{2.1}$  eutectic high-entropy alloys possess bimodal eutectic structures and dendritic phases, with variations in composition significantly affecting the microstructure and mechanical properties [12]. The thermal stability of the intermetallic phases in FeNi alloys also has a crucial effect on determining their mechanical properties at elevated temperatures [13]. Studies have shown that the  $Al_3CuNi$ ,  $Al_7Cu_4Ni$ , and  $Al_9FeNi$  phases exhibit thermal stability up to 350-400°C,

Corresponding author: serdardelice@hitit.edu.tr

<https://doi.org/10.2298/JMMB250721022D>



making them suitable for high-temperature applications [13]. In a previous study, the impact of ternary additions (Al, Co, Cr, Mo, Ta, and Ti) on the sintering behavior, microstructure, and mechanical properties of NiFe-based alloys has been investigated in detail [14].  $\text{Ni}_{40}\text{Fe}_{10}\text{Al}$  and  $\text{Ni}_{40}\text{Fe}_{10}\text{Ti}$  alloys exhibited superior densification and hardness as compared to the other additives. Microstructural analysis revealed that most ternary elements, except for Co and Mo, enhanced densification compared to the binary system. Mechanical investigation indicated that only Al and Ti additions significantly improved hardness [14]. Alloying FeNi with small amounts of non-magnetic or magnetic elements increases the order-disorder transition temperature [15].

Despite extensive research on FeNi-based alloys, the specific influence of Cu additions on their microstructural, mechanical, and magnetic characteristics has not been thoroughly addressed in the literature. The main objective of this work is to systematically investigate how variations in Cu content affect the microstructural evolution, mechanical performance, thermal response, and hyperfine interactions of FeNiCu alloys. By integrating differential scanning calorimetry (DSC), hardness testing, and Mössbauer spectroscopy, this study provides a systematic understanding of how Cu modifies the phase transformation temperatures and enthalpy, hardness, and local magnetic structure. The

novelty of this work lies in establishing a correlation between Cu composition and the simultaneous evolution of thermal and magnetic properties. This may contribute to a deeper understanding of the interrelation between structural, thermal, and magnetic behaviors in FeNiCu alloys.

## 2. Experimental details

FeNiCu alloys were prepared using high-purity (99.9%) elemental powders. The powders were thoroughly mixed and pressed into pellets with a diameter of 1 cm using stainless steel molds. Then, the pellets of the samples were melted in an arc furnace (Edmund Bühler Mini Arc Melter MAM-1). To ensure chemical homogeneity, each sample was re-melted multiple times. The resulting ingots were then homogenized at 1100 °C for 12 hours in vacuum-sealed silica tubes and immediately quenched in iced water. The solidified samples were cut using a precision cutter (Metkon Mikracut 151). The surface of the samples after cutting was exposed to different finer abrasives and polished using 3 µm and 1 µm diamond pastes. Chemical etching was performed using a mixture of 3 ml HF, 40 ml HNO<sub>3</sub>, and 30 ml H<sub>2</sub>O. Schematic diagram of the experimental processes applied to produce FeNiCu alloys was illustrated in Fig. 1. Microstructural and compositional characterization was carried out using a

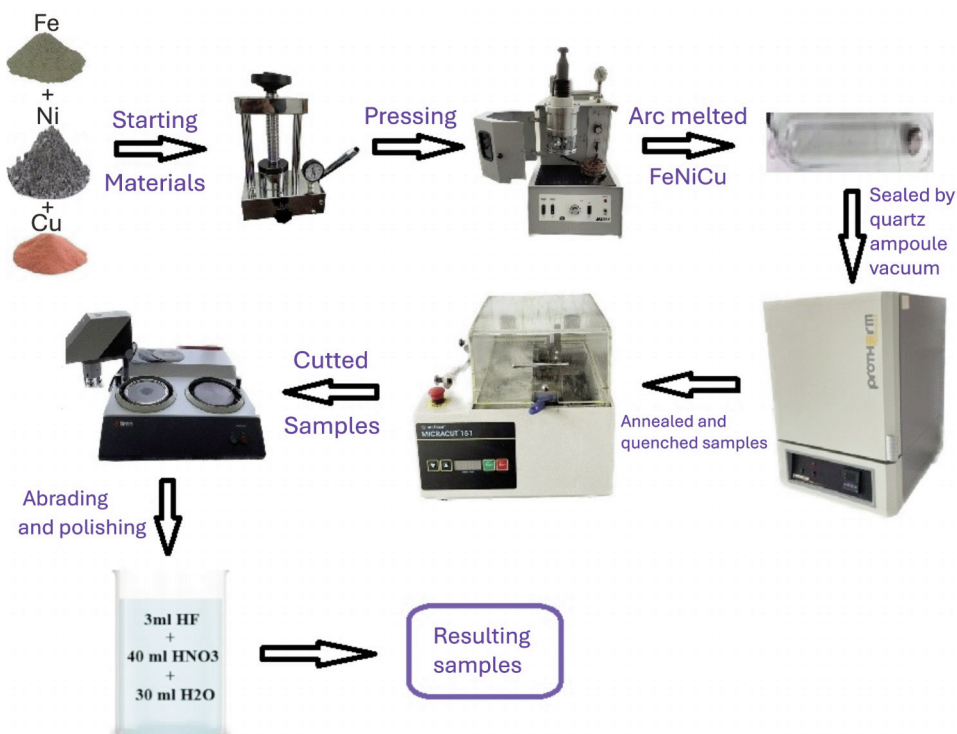


Figure 1. Schematic diagram of the experimental procedure for production of FeNiCu alloy samples

scanning electron microscope equipped with energy-dispersive X-ray spectroscopy (EDX) (FEI Quanta 450 FEG). Elemental compositions of the produced two FeNiCu alloys obtained by the EDX analysis were illustrated in Table 1. Mechanical properties were determined using Vickers microhardness testing with a Metkon Duroline-M instrument. The Vickers hardness tests were performed with an applied load of 2 kgf. Thermal behavior and potential phase transformations were investigated using differential scanning calorimetry. Magnetic properties were studied via room-temperature Mössbauer spectroscopy using a Fast Com Tec PC-moss II system with a <sup>57</sup>Co(Rh) radioactive source. This analysis provided insights into the magnetic hyperfine interactions and atomic-scale phase composition of the alloys.

### 3. Results and discussion

The microstructural analysis of the two Fe-Ni-Cu alloys with different elemental ratios was investigated utilizing SEM micrographs of the prepared surfaces. Figs. 2(a) and (b) illustrate the SEM images of Fe-29.4%Ni-1.54%Cu and Fe-28.35%Ni-2.87%Cu alloys, respectively. As shown in Fig. 2(a), the Fe-29.4%Ni-1.54%Cu alloy presented martensite plates along the matrix. In a previous study, Fe<sub>100-x</sub>Ni<sub>x</sub> alloys were investigated in terms of phase structures [16]. Coexistence of  $\alpha$  and  $\gamma$  phases was confirmed in the alloys. As the concentration of the Ni content

increased the  $\gamma$  phase increased in the structure. At the same amount of Fe and Ni, the  $\gamma$  phase dominated completely [16]. In these alloys, nickel is known to stabilize the austenitic phase [17]. It is well known that Fe-Ni alloys containing between 28 and 30 wt. % Ni can exhibit a face-centered cubic ( $\gamma$ ) structure at room temperature. However, under certain external conditions like plastic deformation, fast cooling, etc., or due to the presence of specific alloying or residual elements, they may undergo a transformation into a body-centered cubic  $\alpha$ -phase with a martensitic ( $\alpha'$ ) structure [18]. In another study, (Fe<sub>85</sub>Ni<sub>15</sub>)<sub>100-x</sub>Cu<sub>x</sub> (x=0, 0.5, 1.5, 3, 5) powders were studied [19].  $\alpha$ -(Fe(Ni-Cu)) solid solution was obtained where Ni and Cu were homogeneously distributed within the matrix. As seen from Fig. 2(a), the Fe-29.4%Ni-1.54%Cu alloy presented a martensite structure within the matrix which can be attributed to the quenching process of the alloy with iced water as compared to the literature works. In the micrograph, there are some pores and scratches which are not related to the microstructural elements but due to the possible reasons during sample preparation. In comparison, the microstructure of the Fe-28.35%Ni-2.87%Cu alloy indicates significant changes as seen in Fig. 2(b), which can be attributed to the relatively lower nickel content and the higher Cu content. The increase in copper leads to an increase in martensite structure observed in the alloy with lower Cu content. Needle-like structure in the micrograph of the Fe-28.35%Ni-2.87%Cu alloy is also observable in the figure. The reduction in nickel content with increasing Cu content may also have modified the transformation temperatures and stability of phases [18], thereby affecting the microstructural characteristics.

The mechanical behavior of both studied alloys was also investigated by employing the Vickers microhardness test method. Hardness testing revealed

**Table 1.** Elemental compositions of the produced FeNiCu alloys

Sample	Fe (wt. %)	Ni (wt. %)	Cu (wt. %)
Sample 1	69.06	29.4	1.54
Sample 2	68.78	28.35	2.87

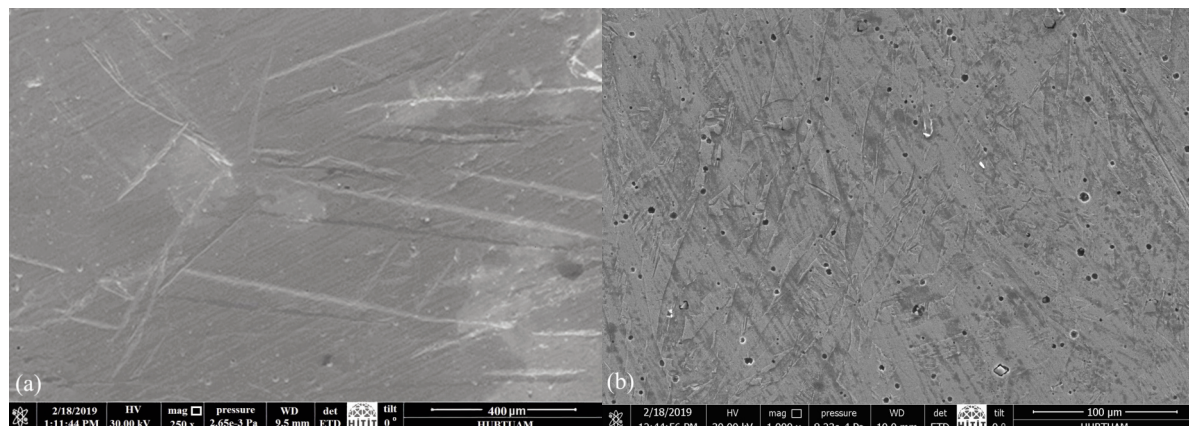


**Figure 2.** SEM images of the FeNiCu alloys produced with different copper contents of (a) 1.54 wt. % and (b) 2.87 wt. %. Martensite plates are observable in both figures. (b) presents also needle-like structures. The amount of martensite structure increased with enhanced Cu content

a significant difference between the two samples. Vickers microhardness values were found to be 169.1 and 190.2 HV for the Fe-29.4%Ni-1.54%Cu and Fe-28.35%Ni-2.87%Cu alloys, respectively. As clearly understood from the analysis, an increase in the Cu content, approximately two times higher in the latter alloy, significantly enhanced the microhardness of the material. The found result seems to be consistent with the SEM analysis, which shows higher martensitic concentration in the matrix for the Fe-28.35%Ni-2.87%Cu alloy. The addition of copper to various alloys has been shown to significantly affect their microhardness. In low-alloy white cast iron, increasing Cu content from 0.5% to 1.5% progressively enhances hardness from 49 HRC to 61 HRC due to the formation of martensitic phases [20]. Our results were consistent with that of the previous work. The observed microhardness increase is primarily dictated by microstructural and compositional effects. The elevated martensite volume fraction in the Fe-28.35%Ni-2.87%Cu alloy is the main contributor to the enhanced bulk hardness. Furthermore, the compositional differences, specifically increasing Cu to Ni ratio in the alloy, may lead to strengthening mechanisms. The Cu atoms may contribute to solid solution hardening and, they may introduce the potential for precipitation hardening by the formation of Cu-rich precipitates [21, 22].

The thermal properties of Fe-29.4%Ni-1.54%Cu and Fe-28.35%Ni-2.87%Cu alloys were also explored using DSC experiments performed at temperatures ranging from room temperature to  $-150^{\circ}\text{C}$  with a constant rate of  $10^{\circ}\text{C}/\text{min}$ . Due to the absence of any variation in the whole recorded DSC curve during cooling, which can indicate some transformations in the structure of samples (e.g., Curie point and/or inter-martensitic), we represented the curves in Fig. 3 in the temperature range between  $-20$  and  $-80^{\circ}\text{C}$ . As seen in Fig. 3(a) and (b), the DSC curves of both alloys exhibited sharp and intense exothermic peaks. The intensity and sharpness of the DSC peak of Fe-28.35%Ni-2.87%Cu were remarkably higher than those of Fe-29.4%Ni-1.54%Cu alloy. The observed DSC peaks strongly suggest the presence of thermo-structural phase transformations at the determined temperature interval. The corresponding martensitic starting ( $M_s$ ) and finishing ( $M_f$ ) temperatures were found from the intersection points of the tangents of onset and endset. Martensitic peak temperatures ( $M_p$ ) was also obtained from the peak maximum temperatures. The  $M_s$ ,  $M_p$  and  $M_f$  values were shown in Fig. 3 and summarized in Table 2. The emitted energies of the transformations during the exothermic process were also indicated in the table. The martensitic transformation temperature of Fe-

28.35%Ni-2.87%Cu was higher than that of Fe-29.4%Ni-1.54%Cu. In a literature work, the effect of Ni concentration on the martensitic transformation temperature of binary FeNi alloys, which were produced by arc melting method, followed by annealing and water quenching, was discussed [23]. A wide range of Ni concentration changing in between 20 at.% and 30 at.% were studied in this paper. It was found that the martensitic transformation temperature decreased dramatically from 500 K ( $\sim 227^{\circ}\text{C}$ ) to 200 K ( $\sim -73^{\circ}\text{C}$ ) as the Ni content was increased from 20 at.% to 30 at.%, respectively. Comparing the concentration ratio of the binary FeNi system to the present study, the martensitic transformation temperature of Fe-30Ni alloy is lower than that of the studied Fe-Ni-Cu alloy with lower Cu content ( $\sim -66^{\circ}\text{C}$ ). In another study, it was shown that the substitution of Cu with Ni increased the martensitic transformation temperature of NiMnSnCu quaternary alloy by stabilizing the austenite phase [24]. Then, the results show that the substituting Cu with Ni increased martensitic transformation temperature in the studied FeNiCu alloys, consisting with the reported literature works. Also, reported results supported the FCC ( $\gamma$ ) to BCC ( $\alpha'$ ) transition during the thermal process [23]. Hysteresis is one of the important phenomenon indicating the transformation features of the materials. However, since the thermal properties of the studied FeNiCu alloys during heating process could not investigated due to insufficient experimental opportunities, we could not determine this parameter. In a study on FeNi alloy, DSC investigation for the heating and cooling process was accomplished and presence of a hysteresis was revealed [25]. As the Ni content increased, the hysteresis value gradually increased. Considering the analogy of our system to the binary FeNi alloy, we may refer to the existence of hysteresis in the studied FeNiCu system. Moreover, as seen from Table 2, the energy released during the transition in the Fe-28.35%Ni-2.87%Cu alloy was almost forty percent higher than that of the Fe-29.4%Ni-1.54%Cu alloy. The enthalpy value increased from 0.56 kJ/mol to 0.77 kJ/mol as the Cu content increased from 1.54 wt. % to 2.87 wt. % as seen in Table 2. This value was previously reported as around 1.1 kJ/mol for FeNi alloy with various Ni concentration value as seen in the table. The enthalpy values of martensitic transformation of  $\text{Ni}_{50-x}\text{Mn}_{36}\text{Sn}_{14}\text{Cu}_x$  alloys ( $x=0, 1$  and  $2$ ) was also reported for Cu substitution for Ni in a previous literature work [24]. In the study, it was indicated that the enthalpy increased from 1.516 J/g ( $\sim 0.1$  kJ/mol) to 2.489 J/g ( $\sim 0.16$  kJ/mol) with increasing Cu up to  $x$ . Comparing the results of present study to those of the reported work in Ref. [24], the increase in the



enthalpy value with increasing Cu content seems reasonable. However, the martensitic transformation energies obtained in the current study are less than those of reported for binary FeNi alloys. The addition of Cu content is likely to have influenced the transformation behavior which may be due to introducing local inhomogeneity that inhibit the martensitic transformation causing the less energy releasing as compared with the binary systems [26].

The insets of the graphs show the first derivative of the observed DSC data with respect to temperature. This mathematical representation is used in thermal analysis to precisely determine the characteristic temperatures of phase transitions, as it amplifies the small changes in the DSC curve [27]. The derivative plots can be used to more accurately determine the onset and endset temperatures of the transformation. The point where the derivative curve first deviates from the baseline points out the start of the transformation. The point where the curve returns to

the baseline level indicates the finish of the transformation. As seen in both figures, the derivative curves display a sharp, distinct minimum. This minimum corresponds to the point of maximum change in the heat flow. The sharpness of the derivative peaks confirmed that the exothermic transformation was rapid and occurred within a very narrow temperature range, which is characteristic of a martensitic transformation. The transformation temperatures determined from the derivative curves were in good agreement with those found from recorded DSC curves. Also, any additional deflection points were not detected in the derivative curves. This indicates that no other transformation event was observed in the alloys at the running temperature interval.

Mössbauer spectrometry can be defined as a sophisticated analytical technique grounded in the recoil-free and resonant absorption and subsequent emission of  $\gamma$ -rays by atomic nuclei that are firmly anchored within a solid matrix. Its utilization is most commonly associated with the isotope iron-57 ( $^{57}\text{Fe}$ ), rendering it a highly valuable tool for the study of iron-containing materials. This method provides detailed information on hyperfine interactions, including isomer shift, quadrupole splitting, and magnetic hyperfine fields. These interactions are directly related to the electronic environment and magnetic properties of the sample. Mössbauer spectroscopy is a highly versatile analytical technique that finds application in a variety of disciplines, including, but not limited to, solid-state physics, metallurgy, mineralogy and materials science. This is due to its sensitivity to even the subtlest changes in atomic and magnetic structures [28, 29]. The instrument possesses a high energy resolution and the capability to probe local atomic environments. These properties make it an essential tool for the

**Table 2.** Phase transition temperatures and emitted energies ( $\Delta H$ ) of Fe-29.4%Ni-1.54%Cu and Fe-28.35%Ni-2.87%Cu alloys. The  $\Delta H$  values extracted from the Ref. [23] was also shown for comparison

Sample	Ms / $^{\circ}\text{C}$	Mp / $^{\circ}\text{C}$	Mf / $^{\circ}\text{C}$	$\text{DH}_{\gamma \rightarrow \alpha'}$ / $\text{kJ mol}^{-1}$
Fe-29.4Ni-1.54Cu (wt. %)	-65.7	-66.3	-69.0	0.56
Fe-28.35Ni-2.87Cu (wt. %)	-48.2	-48.8	-51.1	0.77
Fe-27.4Ni (at.%) [23]	-	-	-	1.4
Fe-28.0Ni (at.%) [23]	-	-	-	1.2
Fe-28.2Ni (at.%) [23]	-	-	-	1.1
Fe-28.8Ni (at.%) [23]	-	-	-	1.1
Fe-29.3Ni (at.%) [23]	-	-	-	1.2
Fe-29.9Ni (at.%) [23]	-	-	-	1.1

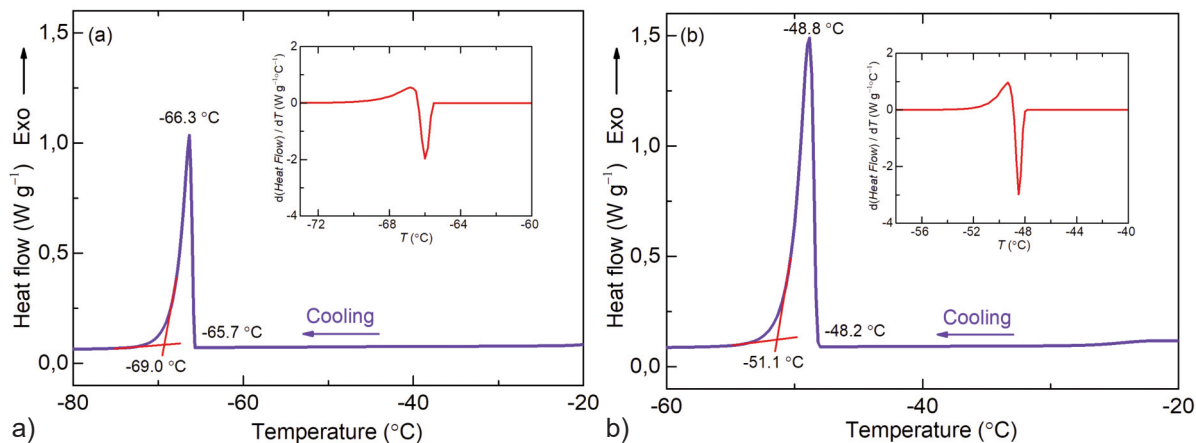


**Figure 3.** DSC peaks of (a) Fe-29.4%Ni-1.54%Cu and (b) Fe-28.35%Ni-2.87%Cu alloys recorded through cooling process. Insets show the first derivative of observed DSC data with respect to temperature

characterization of complex alloys, magnetic phases and nanostructured materials. The presence of certain spectral curves in a Mössbauer spectrum, including singlets, doublets, and sextets, is indicative of particular atomic arrangements. For example, the appearance of a singlet or doublet absorption pattern is indicative of paramagnetic phases and the existence of a sextet absorption pattern reveals the presence of magnetically ordered phases, such as ferromagnetic or antiferromagnetic structures [30].

Mössbauer spectra of the Fe-29.4%Ni-1.54%Cu and Fe-28.35%Ni-2.87%Cu alloys detected at room temperature were depicted in Fig. 4. As seen from Fig. 4(a), the spectrum of the Fe-29.4%Ni-1.54%Cu exhibited a wide and quite asymmetric curve, which was a strong indication that the recorded curve was composed of overlapping Mössbauer structures. The Mössbauer spectrum of the Fe-28.35%Ni-2.87%Cu alloy showed a more symmetric curve with a distinct sextet structure as seen in Fig. 4(b). However, overlapping of all Mössbauer structures existing could also be possible in this spectrum. To find out the observed structures in the spectra, we applied a fit to the experimental data by using the Win Normos fitting program based on the least squares fitting principle. Therefore, it was found that both of the alloys presented the presence of three sextets and one singlet structure in the spectra. The fitting process gave the corresponding Mössbauer parameters of the determined sub-curves successively. The parameters were summarized in Table 3. Compared to the volumetric percentage of formed phases, the Fe-29.4%Ni-1.54%Cu alloy presents approximately 98% magnetically ordered component, while the Fe-28.35%Ni-2.87%Cu alloy exhibited about 94% magnetically ordered structures at room temperature. In iron-based alloys, the austenite phase is related to the paramagnetic structure, whereas the martensite phase corresponds to ferromagnetic structures [30-32]. The observed sextets in the Mössbauer spectra of both alloys are related to different

surroundings of Fe atom in the structure of the samples. The singlet structure observed in both alloys may be associated with the austenite phase. For better understanding the nature of the observed Mössbauer spectra, we handled a comparative study. In literature, there are some Mössbauer studies elucidating the magnetic hyperfine interaction of  $Fe_{100-x}Ni_x$  alloys with varying  $x$  between 10 at.% and 90 at.% [33, 34]. Baldokhin et al. [33] fitted the Mössbauer spectra of FeNi with 10 at.% Ni, which had single BCC phase, by using two sextets and a singlet sub-spectra. The Mössbauer spectra of the alloys with 22 at.% and 28 at.% presenting double phases were also fitted with two sextets and a singlet. The spectra of the alloys having 30 at.% and 50 at.% Ni content had single phase FCC and were fitted with a hyperfine magnetic field distribution. The spectra of the alloys with Ni content above 50 at.% were fitted with three sextets. Valderruten et al. [34] investigated the Mössbauer properties of FeNi alloys with Ni content ranging from 22.5 at.% to 40 at.%. The Mössbauer spectra of all alloys presented two sextets and a singlet. In the both studies, the appearance of the sextets was assigned to the presence of the BCC phases associated with different surroundings of iron atoms [33, 34]. The singlet observed in both study was also attributed to the existence of the FCC paramagnetic Fe-Ni. By the help of similar structural analogy, the singlet observed in the Mössbauer spectra of the present alloys was considered to be due to the presence of the paramagnetic FCC phase in the structure. The internal magnetic field ( $H_{eff}$ ) of the sextet 2 in both alloys was very close to that of  $\alpha$ -Fe (33 T) with negligible variation [35]. However, it significantly deviated from this value for the sextet 1, which possessed the value of around 35 T. This can be due to the strengthening of the magnetic interaction within the ferromagnetic phase, suggesting changes in the local environment of iron atoms. This indicated the existence of two different martensite structures in the alloys. Utilizing from the literature works and experimental data for the  $H_{eff}$ , these

**Table 3.** Mössbauer parameters of Fe-29.4%Ni-1.54%Cu and Fe-28.35%Ni-2.87%Cu alloys. (Q.S: Quadrupole splitting, I.S: Isomer shift, W: Full width at half maximum, Area: Volumetric percentage of phases formed)

Sample	Type	Heff / T ( $\pm 0.04$ )	I.S / mm.s <sup>-1</sup> ( $\pm 0.004$ )	Q.S / mm.s <sup>-1</sup> -0.009	W / mm.s <sup>-1</sup> ( $\pm 0.03$ )	Area / %
Fe-29.4Ni-1.54Cu	Sextet 1	34.932	0.032	-0.076	0.483	6.2034
	Sextet 2	33.185	0.049	0.023	0.291	13.325
	Sextet 3	18.02	0.006	0.014	1.1173	78.11
	Singlet	-	-0.117	-	0.576	2.3609
Fe-28.35Ni-2.87Cu	Sextet 1	34.911	0.035	-0.057	0.462	33.329
	Sextet 2	33.098	0.052	0.025	0.406	34.072
	Sextet 3	18.632	0.053	-0.064	0.646	26.342
	Singlet	-	0.005	-	0.806	6.257



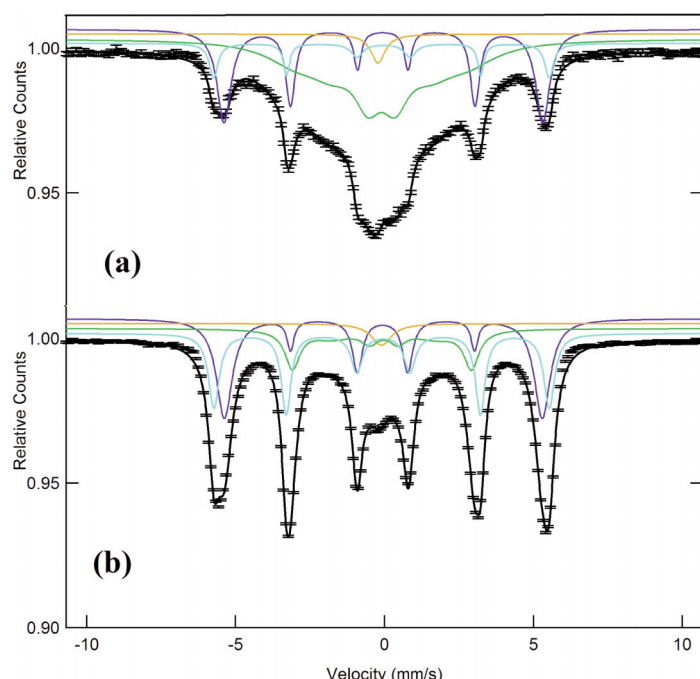


**Figure 4.** Mössbauer spectrum of (a) Fe-29.4%Ni-1.54%Cu and (b) Fe-28.35%Ni-2.87%Cu alloys. Decomposed curves are the curves obtained by fitting the experimental data

two sextets were ascribed to the existence of ferromagnetic BCC structures varying due to different surroundings of Fe atom. One having the  $H_{\text{eff}}$  around 33 T is likely to be Fe-rich phase. The other is possibly due to Fe surrounded by Ni as the nearest neighbour. Further, the  $H_{\text{eff}}$  value of the sextet 3 was dramatically lower as compared to that of  $\alpha$ -Fe, which may be due to a strong change in the local environment of the Fe atom and/or different local atomic distribution with the absence of the Fe atom. Therefore, it may be concluded that this ferromagnetic phase is related to Cu- and/or Ni-rich environments having lower magnetic moment. The isomer shift (I.S.) values of the sextet 3 and the singlet increased with increasing Cu content as seen in Table 3. Such an increase suggested the changes in the s-electron density at the iron atom, which were affected thanks to bonding environments and elemental substitutions [36]. Similarly, the quadrupole splitting (Q.S.) value for the sextet 3 decreased remarkably with increasing Cu content while that of other sextets varied insignificantly. This also indicated the change of local symmetry or electric field gradients around the Fe atom [37].

#### 4. Conclusion

This study investigated the effect of copper addition on the microstructural, mechanical, thermal, and magnetic behaviors of Fe–Ni–Cu alloys. Two compositions, Fe-29.4%Ni-1.54%Cu and Fe-28.35%Ni-2.87%Cu, were synthesized via arc

melting and characterized using SEM, Vickers microhardness testing, DSC, and Mössbauer spectroscopy. SEM micrographs revealed that both alloys exhibited martensitic and austenitic structures. The microhardness results demonstrated a clear strengthening effect. The hardness increased from 169.1 HV to 190.2 HV with higher Cu content. This confirmed that Cu addition refined the microstructure and enhanced mechanical performance. DSC analysis indicated distinct exothermic peaks related to martensitic transformations. The transformation temperatures were  $M_s = -65.7$  °C and  $M_f = -69.0$  °C in the alloy with lower Cu content, whereas those were  $M_s = -48.2$  °C and  $M_f = -51.1$  °C in the alloy with higher Cu concentration. The results indicated that increasing Cu enhanced the transformation temperature. Moreover, this increase in the Cu content led to increase in energy released during martensitic transformation from 0.56 kJ/mol to 0.77 kJ/mol. Mössbauer spectroscopy confirmed the presence of three sextets and one singlet component in both alloys. The weak singlet was attributed to the paramagnetic FCC phase. Among the three sextets, two were associated with ferromagnetic BCC phases arising from different local environments around Fe atoms. The third sextet, characterized by a relatively low internal magnetic field of approximately 18 T, was ascribed to Fe atoms surrounded by Ni- and/or Cu-rich regions, indicating a partial dilution of the magnetic interactions with substitution of Cu in the

alloys. The main scientific contribution of this work is the elucidation of the effects of Cu substitution on the martensitic transformation behavior and hyperfine magnetic interactions in Fe–Ni–Cu alloys, which have not been comprehensively reported previously. These results provide valuable insight into how controlled Cu alloying can be used to tailor both the mechanical strength and magnetic response of Fe–Ni-based systems. The combined improvement in hardness, thermal transformation behavior, and tunable magnetic response suggests that the studied Fe–Ni–Cu alloys are promising for applications requiring both structural stability and controlled magnetic performance. These properties make them suitable for precision instruments, cryogenic components, low-expansion devices, and magnetic sensing and shielding applications where a balance between mechanical strength and magnetic functionality is essential.

### Acknowledgements

*This study was supported by the Scientific Research Projects Coordinatory of Hittit University under the grant number: FEF19002.17.003.*

### Authorship contribution statement

*S. Delice: Writing – original draft, Conceptualization, Formal Analysis, Investigation, Writing - Review & Editing. H. Gungunes: Investigation, Data curation, Formal Analysis, Resources.*

### Data Availability

*Data will be made available on request.*

### Conflict of Interest

*The authors declare that they have no known competing financial interests or personal relationships that could have appeared to influence the work reported in this paper.*

### References

- [1] P. Zhang, L. Li, D. Nordlund, H. Chen, L. Fan, B. Zhang, X. Sheng, Q. Daniel, L. Sun, Dendritic core-shell nickel-iron-copper metal/metal oxide electrode for efficient electrocatalytic water oxidation, *Nature Communications*, 9 (1) (2018) 1–9. <https://doi.org/10.1038/s41467-017-02429-9>
- [2] Y. Geng, X. Lin, Y. Wang, J. Qiang, Y. Wang, C. Dong, Mechanical and magnetic properties of new (Fe,Co,Ni)–B–Si–Ta bulk glassy alloys, *Acta Metallurgica Sinica (English Letters)*, 30 (7) (2017) 659–664. <https://doi.org/10.1007/s40195-017-0576-5>
- [3] X. Qi, J. You, J. Zhou, K. Qiu, X. Cui, J. Tian, B. Li, A review of Fe-based amorphous and nanocrystalline alloys: Preparations, applications, and effects of alloying elements, *Physica Status Solidi A*, 220 (2023) 2300079. <https://doi.org/10.1002/pssa.202300079>
- [4] M.K. Sharma, A. Kumar, K. Kumari, S.-J. Park, N. Yadav, S.-H. Huh, B.-H. Koo, Evidence of hysteresis-free ferromagnetic nature and significant magnetocaloric parameters in FeNi binary alloy, *Magnetochemistry*, 9 (1) (2023) 8. <https://doi.org/10.3390/magnetochemistry9010008>
- [5] B. Aladerah, A. Obeidat, Pressure-dependent magnetic properties of FeNi alloy: theoretical study, *Solid State Sciences*, 148 (2024) 107437. <https://doi.org/10.1016/j.solidstatesciences.2024.107437>
- [6] W. Zheng, Z. Zhou, R. Zou, M. Yang, Enhancing magnetic performance of FeNi<sub>50</sub> soft magnetic composites with double-layer insulating coating for high-frequency applications, *Magnetochemistry*, 10 (7) (2024) 45. <https://doi.org/10.3390/magnetochemistry10070045>
- [7] A. Modak, R. Mohan, K. Rajavelu, R. Cahan, T. Bendikov, A. Schechter, Metal–organic polymer-derived interconnected Fe–Ni alloy by carbon nanotubes as an advanced design of urea oxidation catalysts, *ACS Applied Materials & Interfaces*, 13 (7) (2021) 8461–8473. <https://doi.org/10.1021/acsami.0c22148>
- [8] H. Guo, Z. Chen, J. Li, L. Li, Study of Fe/Ni alloy coated carbon fibres prepared by electroplating, *Surface Engineering*, 35 (10) (2019) 841–847. <https://doi.org/10.1080/02670844.2018.1475103>
- [9] M. Kotsugi, H. Maruyama, N. Ishimatsu, N. Kawamura, M. Suzuki, M. Mizumaki, K. Osaka, T. Matsumoto, T. Ohkochi, T. Ohtsuki, Structural, magnetic and electronic state characterization of L1(0)-type ordered FeNi alloy extracted from a natural meteorite, *Journal of Physics: Condensed Matter*, 26 (6) (2014) 064206. <https://doi.org/10.1088/0953-8984/26/6/064206>
- [10] L. Huang, Y. Zhou, T. Guo, D. Han, Y. Gu, C. Song, F. Pan, Investigation of temperature-dependent magnetic properties and coefficient of thermal expansion in invar alloys, *Materials*, 15 (4) (2022) 1504. <https://doi.org/10.3390/ma15041504>
- [11] A. Sahoo, V.R.R. Medicherla, Fe-Ni invar alloys: A review, *Materials Today: Proceedings*, 43 (2021) 2242–2244. <https://doi.org/10.1016/j.matpr.2020.12.527>
- [12] H. Jiang, L. Li, R. Wang, K. Han, Q. Wang, Effects of chromium on the microstructures and mechanical properties of Al<sub>1-x</sub>Co<sub>x</sub>Cr<sub>y</sub>Fe<sub>2-y</sub> eutectic high entropy alloys, *Acta Metallurgica Sinica (English Letters)*, 34 (11) (2021) 1565–1573. <https://doi.org/10.1007/s40195-021-01303-4>
- [13] F. Meng, Y. Wu, K. Hu, Y. Li, Q. Sun, X. Liu, Evolution and strengthening effects of the heat-resistant phases in Al–Si piston alloys with different Fe/Ni ratios, *Materials*, 12 (16) (2019) 2506. <https://doi.org/10.3390/ma12162506>
- [14] M.B. Shongwe, I.M. Makena, M.M. Ramakokovhu, T. Langa, P.A. Olubambi, Sintering behavior and effect of ternary additions on the microstructure and mechanical properties of Ni–Fe-based alloy, *Particulate Science*



and Technology, 36 (5) (2017) 643–654.  
<https://doi.org/10.1080/02726351.2017.1298686>

[15] L.Y. Tian, O. Gutfleisch, O. Eriksson, L. Vitos, Alloying effect on the order-disorder transformation in tetragonal FeNi, *Scientific Reports*, 11 (2021) 5253.  
<https://doi.org/10.1038/s41598-021-84482-5>

[16] N. Singh, V. Pandey, G. Srivastava, S. Banerjee, O. Parkash, D. Kumar,  $\gamma$  and  $\alpha$ -(Fe,Ni) phase characterization using image processing and effect of phase formation on the P/M  $Fe_{(100-x)}Ni_x$  alloys properties, *Materials Chemistry and Physics*, 246 (2020) 122794.  
<https://doi.org/10.1016/j.matchemphys.2020.122794>

[17] S. Tao, Z. Lu, H. Xie, J. Zhang, X. Wei, Effect of high contents of nickel and silicon on the microstructure and properties of Cu–Ni–Si alloys, *Journal of Micromechanics and Molecular Physics*, 9 (2022) 046516. <https://doi.org/10.1088/2053-1591/ac64ec>

[18] T. Waeckerlé, Low nickel content FCC alloys: recent evolution and applications, *IEEE Transactions on Magnetics*, 46 (2) (2010) 326–332.  
<https://doi.org/10.1109/TMAG.2010.2040465>

[19] A. Abuchenari, M. Moradi, The effect of Cu-substitution on the microstructure and magnetic properties of Fe-15%Ni alloy prepared by mechanical alloying, *Journal of Composites and Compounds*, 1 (1) (2019) 10–15. <https://doi.org/10.29252/jcc.1.1.2>

[20] S.S. Ghasemi Banadkouki, S. Mehranfar, H.R. Karimi Zarchi, Effect of Cu addition on hardness and microstructural features of low alloy white cast iron, *Materials Research Express*, 6 (2018) 026547.  
<https://doi.org/10.1088/2053-1591/aaee48>

[21] Q. Shen, H. Chen, W. Liu, Effect of Cu on nanoscale precipitation evolution and mechanical properties of a Fe–NiAl alloy, *Microscopy and Microanalysis*, 23 (2017) 350–359.  
<https://doi.org/10.1017/S1431927616012599>

[22] H. Sun, D. Li, Y. Diao, Y. He, L. Yan, X. Pang, K. Gao, Nanoscale Cu particle evolution and its impact on the mechanical properties and strengthening mechanism in precipitation-hardening stainless steel, *Materials Characterization*, 188 (2022) 111885.  
<https://doi.org/10.1016/j.matchar.2022.111885>

[23] P. Thome, M. Schneider, V.A. Yardley, E.J. Payton, G. Eggeler, Local maxima in martensite start temperatures in the transition region between lath and plate martensite in Fe–Ni alloys, *Materials*, 16 (2023) 1549.  
<https://doi.org/10.3390/ma16041549>

[24] A. Wederni, M. Ipatov, E. Pineda, J.-J. Suñol, L. Escoda, J. M. González, S. Alleg, M. Khitouni, R. Žuberek, O. Chumak, A. Nabialek, A. Lynnyk, Magnetic properties, martensitic and magnetostructural transformations of ferromagnetic Ni–Mn–Sn–Cu shape memory alloys, *Applied Physics A*, 126 (2020) 320.  
<https://doi.org/10.1007/s00339-020-03489-3>

[25] L.A. Stashkova, N.V. Mushnikov, V.S. Gaviko, A.V. Protasov, Calorimetric studies of phase transformations in Fe–Ni Alloys, *Physics of Metals and Metallography* 123 (2022) 971–978.  
<https://doi.org/10.1134/S0031918X22600907>

[26] R. Wang, G. Qin, E. Zhang, Effect of Cu on martensite transformation of CoCrMo alloy for biomedical application, *Journal of Materials Science & Technology*, 52 (2020) 127–135.  
<https://doi.org/10.1016/j.jmst.2020.04.012>

[27] E. Ghanbari, S.J. Picken, J.H. van Esch, Analysis of differential scanning calorimetry (DSC): determining the transition temperatures, and enthalpy and heat capacity changes in multicomponent systems by analytical model fitting, *Journal of Thermal Analysis and Calorimetry*, 148 (2023) 12393–12409.  
<https://doi.org/10.1007/s10973-023-12356-1>

[28] V.K. Sharma, Z. Homonnay, T. Nishida, J.M. Grenache,  $^{57}Fe$  Mössbauer spectrometry to explore natural and artificial nanostructures, *Journal of Materials Research*, 38 (2023) 925–936.  
<https://doi.org/10.1557/s43578-023-00937-7>

[29] E. Kuzmann, Z. Homonnay, Z. Klencsár, R. Szalay,  $^{57}Fe$  Mössbauer spectroscopy as a tool for study of spin states and magnetic interactions in inorganic chemistry, *Molecules*, 26 (4) (2021) 1062.  
<https://doi.org/10.3390/molecules26041062>

[30] V.J. Angadi, I.S. Yahia, H.Y. Zahran, M.C. Oliveira, E. Longo, S.P. Kubrin, S.O. Manjunatha, R.A.P. Ribeiro, M.H. Ghozza, Effect of  $Eu^{3+}$  on the structural, magnetic and Mössbauer spectroscopy studies of copper ferrite, *Journal of Magnetism and Magnetic Materials*, 562 (2022) 169789.  
<https://doi.org/10.1016/j.jmmm.2022.169789>

[31] D. Ohmer, M. Yi, O. Gutfleisch, B.X. Xu, Phase-field modelling of paramagnetic austenite–ferromagnetic martensite transformation coupled with mechanics and micromagnetics, *International Journal of Solids and Structures*, 238 (2022) 111365.  
<https://doi.org/10.1016/j.ijsolstr.2021.111365>

[32] G.J. Li, E.K. Liu, H.G. Zhang, Y.J. Zhang, J.L. Chen, W.H. Wang, H.W. Zhang, G.H. Wu, S.Y. Yu, Phase diagram, ferromagnetic martensitic transformation and magnetoresponsive properties of Fe-doped MnCoGe alloys, *Journal of Magnetism and Magnetic Materials*, 332 (2013) 146–150.  
<https://doi.org/10.1016/j.jmmm.2012.12.001>

[33] Yu.V. Baldokhin, V.V. Tcherdyntsev, S.D. Kaloshkin, G.A. Kochetov, Yu.A. Pustov, Transformations and fine magnetic structure of mechanically alloyed Fe–Ni alloys, *Journal of Magnetism and Magnetic Materials*, 203 (1999) 313–315. [https://doi.org/10.1016/S0304-8853\(99\)00213-9](https://doi.org/10.1016/S0304-8853(99)00213-9)

[34] J.F. Valderruten, G.A. Pérez Alcázar, J.M. Grenèche, Mössbauer and x-ray study of mechanically alloyed Fe–Ni alloys around the Invar composition, *Journal of Physics: Condensed Matter - IOPscience*, 20 (2008) 485204.  
<https://doi.org/10.1088/0953-8984/20/48/485204>

[35] W.M. Xu, G.R. Hearne, S. Layek, D. Levy, M.P. Pasternak, G.Kh. Rozenberg, E. Greenberg, Interplay between structural and magnetic-electronic responses of  $FeAl_2O_4$  to a megabar: site inversion and spin crossover, *Physical Review B*, 97 (2018) 085120.  
<https://doi.org/10.1103/PhysRevB.97.085120>

[36] G. Comas-Vilà, P. Salvador, Accurate  $^{57}Fe$  Mössbauer parameters from general Gaussian basis sets, *Journal of Chemical Theory and Computation*, 17 (2021) 7724–7731.  
<https://doi.org/10.1021/acs.jctc.1c00722>

[37] Y.V. Knyazev, M.S. Pavlovskii, T.D. Balaev, S.V. Semenov, S.A. Skorobogatov, A.E. Sokolov, D.M. Gokhfeld, K.A. Shaykhutdinov, The effect of  $Mn^{3+}$  substitution on the electric field gradient in a  $HoFe_{1-x}Mn_xO_3$  ( $x = 0–0.7$ ) system, *Crystals*, 14 (2024) 1025.  
<https://doi.org/10.3390/cryst14121025>



## UTICAJ DODATKA BAKRA NA MIKROSTRUKTURU, MEHANIČKA, TERMIČKA I MAGNETNA SVOJSTVA Fe-Ni-Cu LEGURA

Serdar Delice <sup>\*</sup>, Hakan Gungunes

Hitit Univerzitet, Fakultet tehničkih i prirodnih nauka, Katedra za fiziku, Čorum, Turska

### Apstrakt

*U ovoj studiji, FeNiCu legure sa dva različita sadržaja bakra proizvedene su elektrolučnim topljenjem. Cilj istraživanja bio je da se ispita uticaj sadržaja Cu na mikrostrukturna, mehanička, termička i Mosbauerova svojstva legura. Mikrostruktura je ispitivana pomoću SEM mikrografija. Za ocenu mehaničke čvrstoće sprovedena su ispitivanja Vikersove tvrdoće. Termičko ponašanje analizirano je primenom DSC metode. Magnetne karakteristike proučavane su Mosbauerovom spektroskopijom. SEM analiza je pokazala prisustvo martenzitnih struktura u obe legure, pri čemu je legura sa većim sadržajem Cu pokazala veći udeo martenzita. Tvrdoća je porasla sa 169,1 HV na 190,2 HV sa povećanjem sadržaja Cu. DSC rezultati su potvrdili martenzitnu transformaciju. Legura sa većim sadržajem Cu pokazala je višu temperaturu transformacije i veću energiju oslobođenju tokom transformacije. Mosbauerovi spektri ukazali su na prisustvo magnetno uredenih i neuređenih faza u obe legure. Hiperfini parametri ukazali su na promene u lokalnom atomskom okruženju usled dodatka Cu. Dobijeni slabi singlet je povezan sa FCC fazom. Dva seksteta pripisana su feromagnetskim BCC fazama koje potiču iz različitih okruženja Fe atoma. Treći sekstet, sa niskim internim magnetnim poljem od oko 18 T, pripisan je mogućem Ni- i/ili Cu-bogatom okruženju Fe atoma. Sve u svemu, povećanje Cu u leguri je izmenilo mikrostrukturu, poboljšalo tvrdoću, pomerilo temperaturu martenzitne transformacije i modifikovalo magnetne hiperfine interakcije. Ovi rezultati mogu pomoći u dizajniranju naprednih materijala na bazi Fe za strukturne i magnetne primene.*

**Ključne reči:** FeNiCu; SEM; Vikersova tvrdoća; DSC; Mosbauerov efekat

